

⁵D. J. Jackson, J. J. Wynne, and P. H. Kes, to be published.

⁶N. Bloembergen, *Nonlinear Optics* (Benjamin, New York, 1965), pp. 74–83.

⁷C. R. Vidal, *Appl. Opt.* **19**, 3897 (1980).

⁸R. P. Feynman, F. L. Vernon, Jr., and R. W. Hellwarth, *J. Appl. Phys.* **28**, 49 (1957); D. Grischkowsky, *Phys. Rev. A* **7**, 2096 (1973).

Effect of a Static Electric Field on the Trapping of Beam Electrons in a Slow Wave Structure

S. I. Tsunoda and J. H. Malmberg

Department of Physics, University of California, San Diego, La Jolla, California 92093

(Received 3 May 1982)

The effect of an applied static electric field on trapped beam electrons in a traveling wave tube has been observed. In particular, it was found that the wave power can be increased. It was found that beam space charge can play an important role in limiting the wave-power enhancement, and that the wave enhancement is strongly dependent on the rf input drive level. By launching large-amplitude waves over 10 dB of enhanced wave growth has been observed.

PACS numbers: 41.70.+t, 42.60.-v, 52.40.Mj, 85.10.Hy

In a previous Letter¹ it was predicted that if an external force is applied to particles executing nonlinear trapping oscillations in a plasma wave, the wave power can be increased. We have observed this effect in a traveling wave tube² (TWT). The equations³ that describe the wave-particle interaction in a TWT are identical to those^{4,5} that describe the beam-plasma instability in the small-cold-beam limit. The effect of a static electric field on trapped beam particles has been studied theoretically both in a small-cold-beam-plasma system and in a TWT. In the beam-plasma system the theory was first done by Morales.¹ In the TWT, it was done by Hess.⁶

Although the physics of this effect in this highly nonlinear system is interesting in and of itself, there are more practical reasons for studying it as well. One of the reasons that motivates the study of this effect in the beam-plasma case is that it provides a possible model for the interaction of runaway electrons with cavity modes in a tokamak.¹ The study of this effect in the TWT case is motivated by the possibility of enhancing⁷ the wave growth past saturation in TWT's. Indeed, a closely related enhancement technique, velocity tapering, has been well studied⁷ theoretically and experimentally. In addition, because of the analogy between free-electron lasers and TWT's, recent ideas⁸ concerning power enhancement in free-electron lasers may also stimulate interest in the study of this effect.

The main qualitative features of the effect can

be understood by considering the following simplified physical picture. If a weak force is applied to particles trapped in the potential well of a wave of essentially fixed phase velocity, the response of the particles cannot be a uniform acceleration because they are constrained to move on the average at the wave phase velocity. Since the particles cannot change their momentum in response to the applied force, the wave responds by changing its momentum. And because the wave power is proportional to the wave momentum, the wave power can be increased in this way. If the applied force is strong enough to detrap the particles, the particles accelerate, and the wave-power enhancement is destroyed.

We have observed these effects in a TWT. The effects are also predicted by our computer simulations and the computer solutions agree well with the experiment. The apparatus, which has been described elsewhere,⁹ differs from most conventional TWT's in that it is 3–4 times longer when measured in scaled units. A cold electron beam is directed down the axis of a wire helix slow wave structure which is held together by a support structure and is enclosed by a glass vacuum tube. Outside of the glass tube are electrostatic probes which are used to transmit and receive radio-frequency waves. This assembly is enclosed by a grounded cylindrical conductor which is slotted so that the probes can be moved axially. The grounded cylinder acts as a waveguide beyond cutoff and insures that waves

launched by the transmitting probe propagate only along the helix. The applied static electric field is produced by grounding the end of the helix that is near the electron gun and applying a potential to the end near the collector. Thus, the applied field extends through both the linear and nonlinear interaction regions of the tube. This potential is pulsed to avoid overheating the helix structure. The time variation of the pulse is much slower than the electron transit time so that at any instant all the electrons in the interaction region feel an essentially uniform, static applied field. In addition, since ions can be produced by collisions between beam electrons and the residual gas background, the beam is pulsed to avoid beam neutralization.

The existence of the effect is demonstrated by the plots of wave power versus axial distance in Figs. 1 and 2. The solid curve in Fig. 1 represents the axial variation of wave power with no static electric field present. The wave power grows exponentially up to saturation and then executes three trapped-particle oscillations. The fast oscillations represent a beat between the forward wave and a small reflected backward wave due to imperfectly matched ends. The backward wave does not interact significantly with the electrons since it is far from synchronism with the beam. The slight damping which is evident is due to dissipation in the support structure of the wire helix. The dotted curve in Fig. 1 shows the axial power variation in the presence of a

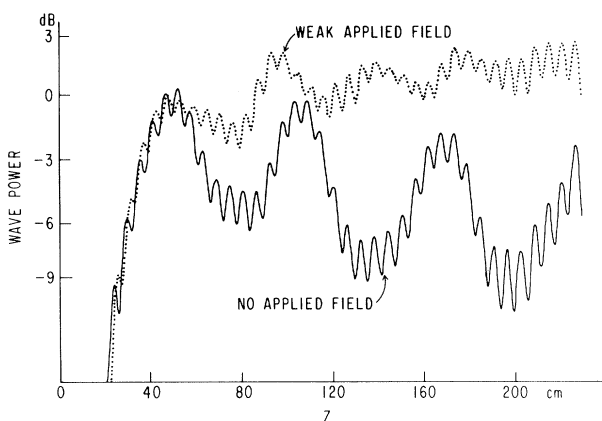


FIG. 1. Wave power vs axial distance. The beam current $I_0 = 1.1$ mA. The frequency $f = 40.0$ MHz. 0 dB corresponds to 30.9 mW. For the case with no static field applied (solid line) the beam voltage $V_0 = 97.4$ V. For the weak applied field case (dotted line), $V_0 = 85.8$ V, $E_{dc} = 0.535$ V/cm.

weak static field. The direction of the field is such that it would accelerate the electrons in the absence of the wave. The wave power grows up to an initial saturation level and then continues to grow about 3 dB past saturation. In both Figs. 1 and 2 the initial beam velocities have been adjusted so that at the position where saturation occurs the power in both cases is the same. The dotted curve in Fig. 2 is a plot of the axial power variation when a strong field is applied. The wave grows through the linear region and saturates but then no appreciable wave-power enhancement occurs.

A useful way to characterize these power plots is to calculate an average slope in the nonlinear region. In the simplified case of zero damping conservation of momentum in the initial beam frame suggests that when the beam is completely trapped the wave power averaged over many trapping oscillations should increase linearly with distance when the static field is applied. The first step in the data analysis is to consider just the nonlinear region and use the measured cold-circuit damping value to adjust the plots for the attenuation due to the dissipation in the helix support structure. Next, the data are put on a linear scale and Fourier analyzed. The trapping oscillations are numerically filtered out, and the result is inverse Fourier transformed. Finally, the slope of the resulting smoothed curve is calculated by a least-squares fit. The slope thus obtained is found to be essentially independent of the type of numerical filter used.

Our computer solutions are essentially solutions of the equations of Tien³ for the parameters

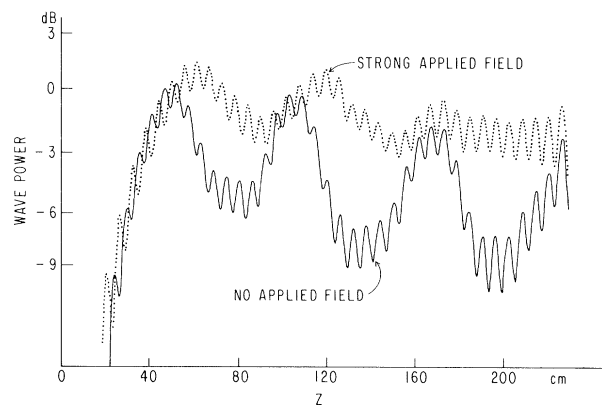


FIG. 2. Wave power vs axial distance. For the strong applied field case (dotted line), $V_0 = 112$ V, $E_{dc} = 0.665$ V/cm. All other parameters are the same as in Fig. 1.

of the experiment. The model includes detuning, damping, finite-beam-strength corrections, and space charge (i.e., the Coulomb force between beam electrons). The important differences between this model and that of Morales are the inclusion of beam space charge and the presence of the applied field in both the linear and nonlinear regions of the tube instead of only in the nonlinear region as assumed by Morales.

In Fig. 3 we exhibit the dependence of the slope of the wave-power plots on the strength of the static electric field. The static electric field, E_{dc} , is applied along the entire length of the helix including the region before trapping has occurred. The computed points are solutions of the equations for 100 particles and are analyzed in exactly the same way as the experimental data. The solid points represent the experimental data. The open circles represent the computed results with space charge included. One of the differences between our TWT and a small-cold-beam-plasma system is that the beam space-charge forces in the TWT are much greater than in the small-cold-beam-plasma system. The open triangles represent the computer solutions when space charge is not included. The experimental results agree well with the calculations including space charge but disagree with the calculations not including space charge. Our computer studies have shown that in the latter case the electrons

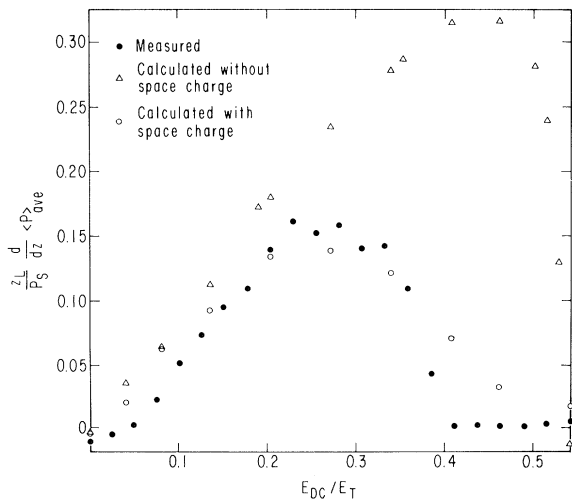


FIG. 3. Scaled secular growth rate vs applied static field. E_{dc} is scaled to the wave field at saturation, $E_T = 0.685$ V/cm. The wave power, P , is scaled to the saturation power, $P_s = 0.775$ mW. The axial distance, z , is scaled to the linear e -folding distance, $z_L = 11.3$ cm. $V_0 = 42.6$ V, $I_0 = 0.10$ mA, and $f = 60.0$ MHz.

near the edge of the potential well can easily decelerate towards the center of the well. In the former case the motion of the electrons toward the center is slowed down. These electrons are more susceptible to detrapping and many of them become runaway electrons.

The wave enhancement can be increased by increasing the input rf drive level. In Fig. 4 we plot the scaled secular growth rate versus the scaled applied field strength for four different values of input rf drive level. The solid symbols are the experimental results and the open symbols are the corresponding results of the simulation. The data labeled SAT correspond to an rf drive level near the saturation amplitude. The data labeled SAT - 2.6, SAT - 13, and SAT - 26 correspond to launched levels 2.6, 13, and 26 dB below the SAT drive level. The solid lines are drawn in only to aid the eye in following the trend of the data points. In Fig. 5 we show a case of over 10 dB of enhanced growth. The wave has been launched near saturation. The ordinate is linear in power. The dashed curve indicates the saturation power level, P_s . Finally, we note that the application of the static electric field increases the efficiency of the TWT. In the absence of a static electric field, the amplifier efficiency is given by $P_s / I_0 V_0$ and for the values of Fig. 5 is 19.2%. In the presence of the static field, the amplifier efficiency is $P / [I_0 (V_0 + V_H) + P_s]$, and for the Fig. 5 values is 37.5%.

In conclusion, we have observed the effect of a

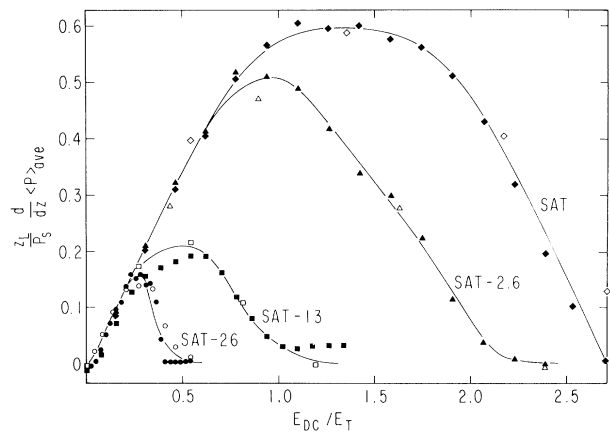


FIG. 4. Scaled secular growth rate vs scaled applied static field for various input rf drive levels. Open symbols are the simulation results and solid symbols are the experimental results. Except for the value of input rf drive level (see text), all parameters are the same as in Fig. 3.

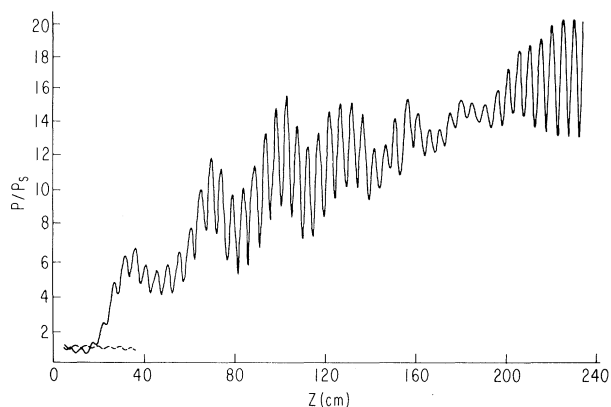


FIG. 5. Wave power (linear scale) vs axial distance. The launched wave amplitude is near the saturation level which is marked by the dashed line. $V_0 = 55.7$ V, $I_0 = 0.50$ mA, $f = 45.0$ MHz, $E_{dc} = 1.88$ V/cm, and $P_s = 5.36$ mW. The applied static voltage $V_H = 506$ V.

static electric field on beam trapping in a TWT. For weak fields the wave power can be enhanced while for stronger fields beam detrapping occurs and the enhancement diminishes. Space charge can play an important role in causing the beam to be detrapped. The wave enhancement has been found to be strongly dependent on the rf input drive level. In particular, appreciable wave en-

hancement of launched large-amplitude waves has been observed.

We wish to thank Professor N. M. Kroll for useful discussions. This work was supported by the National Science Foundation under Grant No. PHY80-09326.

¹G. J. Morales, Phys. Rev. Lett. **41**, 646 (1978).

²J. R. Pierce, *Traveling Wave Tubes* (Van Nostrand, New York, 1950).

³P. K. Tien, Bell Sys. Tech. J. **35**, 349 (1956).

⁴T. M. O'Neil, J. H. Winfrey, and J. H. Malmberg, Phys. Fluids **14**, 1204 (1971); T. M. O'Neil and J. H. Winfrey, Phys. Fluids **15**, 1514 (1972).

⁵I. N. Onischenko, A. R. Linetskii, N. G. Matsiborko, V. D. Shapiro, and V. I. Shevchenko, Pis'ma Zh. Eksp. Teor. Fiz. **12**, 407 (1970) [JETP Lett. **12**, 281 (1970)].

⁶R. L. Hess, Ph.D. thesis, University of California, 1960 (unpublished).

⁷J. E. Rowe, *Nonlinear Electron-Wave Interaction Phenomena* (Academic, New York, 1965).

⁸N. M. Kroll, P. Morton, and M. N. Rosenbluth, *Free Electron Generators of Coherent Radiation* (Addison-Wesley, Reading, Mass., 1980), Chaps. 4, 5, and 6.

⁹G. Dimonte and J. H. Malmberg, Phys. Fluids **21**, 1188 (1978).

Measurements of Enhanced Stopping of 1-MeV Deuterons in Target-Ablation Plasmas

F. C. Young, D. Mosher, S. J. Stephanakis, and Shyke A. Goldstein^(a)
Naval Research Laboratory, Washington, D. C. 20375

and

T. A. Mehlhorn
Sandia National Laboratory, Albuquerque, New Mexico 87115
 (Received 28 April 1982)

Enhancement of the energy loss of 1-MeV deuterons in target-ablation plasmas over that in cold targets has been observed when significant ionization is present in the plasma. Scaling of enhanced stopping with target ionization is consistent with stopping by free electrons and the remaining bound electrons. Measured energy losses for Mylar and aluminum targets are also in agreement with hydrocode calculations.

PACS numbers: 52.40.Mj, 29.70.Gn, 52.50.Gj, 52.70.Nc

Inertial confinement fusion (ICF) with ion-beam drivers requires high-power-density deposition of ion energy in fusion targets. The beam power density is proportional to the current density focused onto the pellet target and to the stopping power of the beam-heated target material. Cal-

culations¹⁻³ indicate that at the ionization levels of ICF pellet plasmas, the ion stopping power is enhanced such that the ion range is about half of that in a cold target. In this paper, measurements of the energy loss of megaelectronvolt deuterons in plasmas formed by focusing the beam